

Normal-state pseudogap in $\text{Bi}_2\text{Sr}_2\text{CaCu}_2\text{O}_8$ characterized by impurity scattering

J. L. Tallon

New Zealand Institute for Industrial Research, P.O. Box 31310, Lower Hutt, New Zealand

(Received 7 April 1998)

A major difficulty in resolving the discrepancies between angle-resolved photoemission spectroscopy (ARPES) studies on the normal-state pseudogap and high-precision electronic heat capacity and NMR measurements has been that the ARPES results are exclusively for $\text{Bi}_2\text{Sr}_2\text{CaCu}_2\text{O}_8$ while the heat capacity and NMR data are primarily for $\text{La}_{2-x}\text{Sr}_x\text{CuO}_4$ and $\text{Y}_{1-x}\text{Ca}_x\text{Ba}_2\text{Cu}_3\text{O}_{7-\delta}$. Here we determine the density of states near the Fermi energy for $\text{Bi}_2\text{Sr}_2\text{CaCu}_2\text{O}_8$ from the impurity depression of T_c and using the scaling behavior of the spin susceptibility and entropy above and below T_c we are able to generate the full temperature dependence of these quantities in the normal and superconducting states. The detailed behavior is almost identical to that for $\text{Y}_{1-x}\text{Ca}_x\text{Ba}_2\text{Cu}_3\text{O}_{7-\delta}$ showing that the direct comparison of these two cuprates is valid.
[S0163-1829(98)50434-1]

In the past year striking results have been reported from ARPES studies on single crystals of $\text{Bi}_2\text{Sr}_2\text{CaCu}_2\text{O}_8$ (Bi-2212) showing that the underdoped region is characterized by heavily damped quasiparticles near the zone boundary¹ and the appearance of an anisotropic gap in the charge spectrum^{2,3} corresponding to the pseudogap previously reported from NMR, neutron scattering, heat capacity, infrared, and transport studies.⁴ While these ARPES studies served to catalyze increased theoretical attention on the pseudogap⁵ several of the key results had been earlier anticipated in high-precision differential heat capacity studies showing that the pseudogap develops in the total excitation spectrum with spin and charge degrees of freedom freezing out simultaneously forming a gap which is anisotropic in k space and linear in energy near the chemical potential.⁶⁻⁹ These conclusions were drawn from studies on $\text{La}_{2-x}\text{Sr}_x\text{CuO}_4$ (La-214),⁶ $\text{Y}_1\text{Ba}_2\text{Cu}_3\text{O}_{7-\delta}$ (Y-123) (Ref. 7) and $\text{Y}_{1-x}\text{Ca}_x\text{Ba}_2\text{Cu}_3\text{O}_{7-\delta}$ (Y:Ca-123) (Ref. 9) and confirmed in detail by NMR studies on the same materials.¹⁰⁻¹² There are, however, key points of tension between the ARPES and heat capacity studies that are critical for some models.^{12,13} The leading-edge analysis of the ARPES data suggests that the pseudogap evolves smoothly from the superconducting gap with the gap energy falling steadily to zero well above T_c in strongly underdoped Bi-2212.^{2,3} This concurs with several models which view the pseudogap as some form of precursor pairing which sets in at a mean-field transition temperature T^* above T_c and develops into long-range phase coherence at T_c .^{14,15} In contrast, the heat capacity and NMR results show the pseudogap and superconductivity to be independent and competing to the lowest temperatures with a discontinuous change in slope in the gap energy $\Delta(T)$ at T_c to preserve the second-order character of the transition and a relatively temperature-independent normal-state gap $\Delta(T) = E_g$.¹² Any marked temperature dependence in E_g would result in a strong temperature dependence of γ , the linear coefficient in the heat capacity that simply is not present.

While the resolution of these differences is critical to developing a satisfactory model for the high-temperature superconducting (HTS) cuprates a lingering doubt remains in that the subject materials for the ARPES on the one hand and

heat capacity and NMR on the other are different. The latter techniques have not been applied to Bi-2212. Pending such studies the present paper takes another tack. It has recently been shown that the depression in T_c due to impurity substitution can be quantitatively understood in terms of unitarity-limit scattering for a d -wave order parameter in the presence of a pseudogap competing with superconductivity down to $T=0$.¹⁶ The only input required is the value of S/T at T_c where S is the entropy. Here we reverse the process and deduce the value of $(S/T)_{T_c}$ from the impurity depression of T_c . Moreover, using the observed scaling behavior of the spin susceptibility χ_s and S/T above and below T_c this is sufficient to determine the entire T dependence of these quantities in the normal and superconducting states. The resulting curves and variation of the pseudogap energy E_g with hole concentration are found to be quantitatively almost the same as found for Y-123 from direct thermodynamic measurements.

Impurity scattering. The impurity-induced depression of T_c and of superfluid density has been shown from muon spin relaxation (μSR) measurements to be quantitatively consistent with scattering in the unitarity limit for a d -wave order parameter.¹⁷ We note that, with the exception of Y-123 in which Ni also occupies the CuO chain sites, the explicit reduction in T_c with impurity concentration z for HTS cuprates is more or less the same for both Zn and Ni.^{16,18} The reduction $T_c(z, p)$ varies strongly with the hole concentration p and is remarkably reproduced by the unitary scattering model with no adjustable parameters subject to two conditions: incorporation of strong coupling and of the pseudogap.

The reduction in T_c for elastic scattering in weak-coupling d -wave superconductors is given by the Abrikosov-Gor'kov (AG) equation.¹⁹ Use of this equation for the very short coherence length cuprates has been justified elsewhere.¹⁶ Thus

$$-\ln(T_c/T_{co}) = \psi[\frac{1}{2} + \Gamma/(2\pi k_B T_c)] - \psi[\frac{1}{2}], \quad (1)$$

where $\psi[x]$ is the digamma function, $T_{co} = T_c(z=0)$, and for unitary scattering $\Gamma = n_i/\pi N(E_F)$ is the pair-breaking scattering rate. Here $N(E_F)$ is the density of states (DOS) per

spin at the Fermi level and $n_i (= \alpha z_{ab}/abc)$ is the volume density of impurity scatterers with z_{ab} being the concentration of impurity atoms in the CuO_2 plane, α being the number of CuO_2 planes per unit cell and a , b , and c being the lattice parameters. For example, for $\text{La}_{2-x}\text{Sr}_x\text{Cu}_{1-z}\text{Zn}_z\text{O}_4$ $\alpha=1$ and $z_{ab}=z$, for $\text{Bi}_2\text{Sr}_2\text{CaCu}_{2(1-z)}\text{Zn}_{2z}\text{O}_8$ $\alpha=2$ and $z_{ab}=z$, while for $\text{Y}_1\text{Ba}_2\text{Cu}_{2(1-z)}\text{Zn}_{3z}\text{O}_{7-\delta}$ $\alpha=2$ and $y_{ab}=3y/2$ because Zn only occupies the CuO_2 plane site. As noted, this model is for *weak coupling* and the critical scattering rate at which T_c is reduced to zero is $\Gamma_c = 0.88k_B T_{co} = 0.412\Delta_{oo}$. This implicitly contains the weak-coupling ratio $2\Delta_o/k_B T_c = 4.28$. However the experimental observation^{20,21,9} is of *strong coupling* with $2\Delta_o/k_B T_c \approx 8$ and it was argued that in such a regime it is Δ_{oo} , not T_{co} , which sets the energy scale for pair breaking¹⁶ so that $\Gamma_c = 0.412\Delta_{oo} = 1.65k_B T_{co}$. This provides a slower suppression of T_c than in the weak-coupling case. Finally, the DOS may be determined from the temperature coefficient of the heat capacity, $\gamma = C_V/T$ using

$$\gamma = (2/3)\pi^2 k_B^2 N(E_F). \quad (2)$$

As a consequence of these relations the initial slope, dT_c/dz_{ab} , is given by

$$dT_c/dz_{ab} = -7.32\alpha/\gamma_{T_c} \quad (3)$$

where $\gamma_{T_c} = \gamma(T=T_c)$ is in units of J/mol.K². Experimentally one finds that the normal-state γ at T_c remains more or less constant in the overdoped region ($=1.9$ mJ/g atoms K² for $\text{Y}_{0.8}\text{Ca}_{0.2}\text{Ba}_2\text{Cu}_3\text{O}_{7-\delta}$) and falls sharply on the underdoped side due to the opening of the pseudogap. This means that the initial slope of the depression in T_c is constant, independent of p and T_{co} in the overdoped region where the pseudogap is absent and diverges in the underdoped region with the appearance of the pseudogap. As an effective value of γ we took $\langle \gamma \rangle_{T_c} = S/T$ at T_c , since S/T is the average value of γ between 0 and T . This model gave an excellent description of the experimental data $T_c(z_{ab}, p)$ for Zn substitution in Y:Ca-123, Y-124, and La-214.

Thermodynamic scaling. Under the assumption that there are well-defined quasiparticles in the neighborhood of the Fermi surface the susceptibility and entropy may be modeled from the DOS using²²

$$\chi_s = 2\mu_B^2 \int [-\partial f(E)/\partial E] N(E) dE \quad (4)$$

and

$$S = -2k_B \int [f \ln f + (1-f) \ln(1-f)] N(E) dE, \quad (5)$$

where $f(E) = [\exp(-E/k_B T) + 1]^{-1}$ is the Fermi function. The Fermi windows for each of these are very similar so that S/T and χ_s are predicted within this model to have nearly the same temperature dependences. This is observed experimentally and the ratio $\chi_s T/S$ over a wide range of temperature and doping is found to be very close to the Wilson ratio for freely interacting fermions.⁸ This at least partially justifies the model. It is by now well established that the superconducting order parameter has *d-wave* symmetry: $\Delta_o(\mathbf{k})$

$= \Delta_o \cos(2\theta)$ while the pseudogap appears to have phaseless “*d-wave-like*” symmetry: $E_g(\mathbf{k}) = E_g |\cos(2\theta)|$. Under such circumstances it has been shown that the temperature dependence of χ_s and S/T above and below T_c follow a simple scaling behavior whatever the doping, such that a universal function is recovered if T is scaled by E_g above T_c or by Δ_o below T_c .^{11,12} This was shown to be satisfied by a wide range of cuprates over a wide range of doping. Thus $\chi_s(T) = \mu_B^2 N_o X(y)$, where

$$X(y) = \int g(x) \text{sech}^2(x/y) y^{-1} dx, \quad (6)$$

with $y = 2k_B T/E_g$, $g(x = E/E_g) = N(E)/N_o$, and N_o is the underlying two-dimensional DOS in the absence of the pseudogap. Similarly, $S/T = 4k_B^2 N_o \Sigma(y)$, where

$$\Sigma(y) = - \int g(x) [f \ln f + (1-f) \ln(1-f)] y^{-1} dx, \quad (7)$$

where $f \equiv f(2x/y) \equiv f(E/k_B T)$. Equation (6) was shown to be satisfied in the normal state for Y-123, (Y,Ca)-123, Y-124, Y-247, La-2126, Tl-2212, Hg-1201, and Hg-1223.¹² Below T_c universal curves were obtained using the scaling parameter $z = 2k_B T/\Delta_o$, however scaling could not be accomplished simultaneously above and below T_c indicating that the two energy scales Δ_o and E_g are independent.

Impurity substitution for Cu in Bi-2212 has been extensively studied by Kluge *et al.*²³ using Zn, Ni, Co, and Fe. Zn and Ni both have low solubility limits, Zn being lower than 1% and it is difficult therefore to establish reliably the initial slope for this substituent. The others, however, exhibit a common specific reduction in T_c so we focus on Co which appears to be soluble to levels higher than 10% and for which the data are rather uniform. Hole concentrations were varied by changing the oxygen content through annealing and the underdoped region was accessed by carrying out similar studies on $\text{Bi}_2\text{Sr}_2\text{Ca}_{0.7}\text{Y}_{0.3}\text{Cu}_{2-2z}\text{Co}_{2z}\text{O}_8$ where the Y substitution is effective in reducing p . The determination of p for Bi-2212 is made difficult by the twin effects of oxygen nonstoichiometry and mixed valancy of Bi. To analyze their data we elect to simply convert T_c values to p values using the parabolic relation

$$T_c/T_{c,\max} = 1 - 82.6(p - 0.16)^2, \quad (8)$$

which is found to approximate many of the cuprates.²⁴ Additional support for this assumption comes from the fact that it is consistent with the correlation of thermoelectric power with hole concentration satisfied by the cuprates,²⁵ namely that different cuprates with the same ratio of $T_c/T_{c,\max}$ have the same room-temperature thermoelectric power. Figure 1 shows T_c plotted versus p for $\text{Bi}_2\text{Sr}_2\text{CaCu}_{2-2z}\text{Co}_{2z}\text{O}_8$ with $z = 0, 1, 2, 4, 6, 8$, and 10%. As for Y-123 and La-214 the approximately parabolic curves collapse asymmetrically to higher values of p towards the point $p = 0.19$ where (in Y:Ca-123) $E_g \rightarrow 0$. Figure 2 shows the explicit dependence of T_c plotted as a function of Co content for each of the oxygen (or hole) concentrations investigated. This shows a series of data curves $T_c(z)$ extending down from a value $T_{co} = T_c(z = 0)$ which, with increasing p , rises to a maximum $T_{co} = 93$ K at optimal doping then falls on the overdoped side.

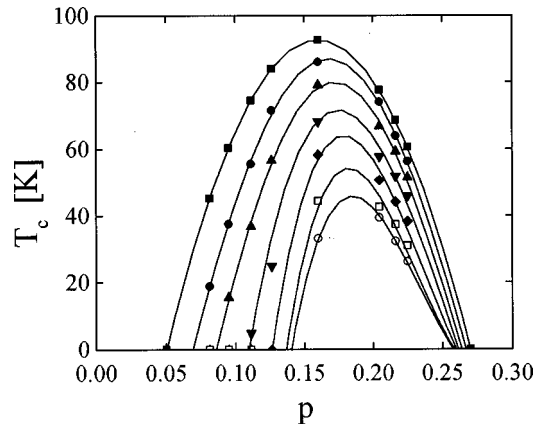


FIG. 1. T_c plotted as a function of hole concentration p for Bi-2212 with 0, 1, 2, 4, 6, 8, and 10% Co substitution for Cu.

Filled symbols with solid lines denote overdoped samples and open symbols with dashed curves denote underdoped samples. Here, as for Y:Ca-123 and La-214, the overdoped region shows a series of curves progressively moving down in parallel, while, beginning already with the optimally-doped samples ($p=0.16$) and extending into the underdoped region, the data $T_c(z)$ falls progressively more rapidly due to the opening of the pseudogap.

Our approach, now, in analyzing these data is to fit each data set to the Abrikosov-Gor'kov Eq. (1) (placing more emphasis on the lower substitution levels) resulting in the solid and dashed curves shown in the figure. From the critical concentration for each we determine the value of S/T at T_c and finally, from this value we generate the full temperature dependence, shown in Fig. 3, of S/T above and below T_c using the scaling relations and universal curve given by Eq. (7). Equally, $\chi_s(T)$ may be generated in the same manner resulting in a very similar set of curves. Several points are notable. (i) The pseudogap is evidently absent in the overdoped region where S/T is essentially T and p independent with the value 2.05 mJ/g atoms K^2 , which is very similar to the value 1.9 mJ/g atoms K^2 experimentally observed for Y:Ca-123. This is the value predicted also for $\gamma(T)$ in this region. (ii) The optimally doped sample already exhibits a

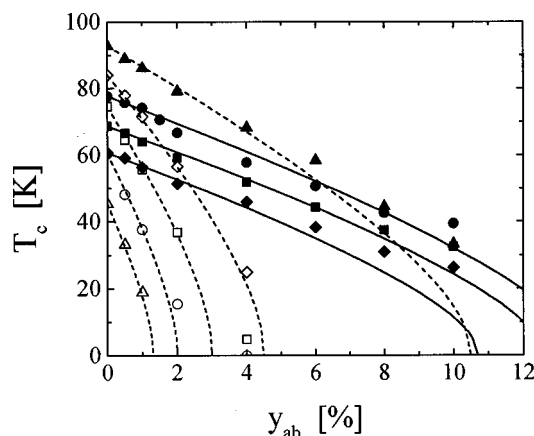


FIG. 2. Constant-hole-concentration plots of T_c as a function of Co substitution. Open symbols and dashed curves denote underdoped samples. Filled symbols and solid curves denote overdoped samples. The curves are the fitted Abrikosov-Gor'kov equation.

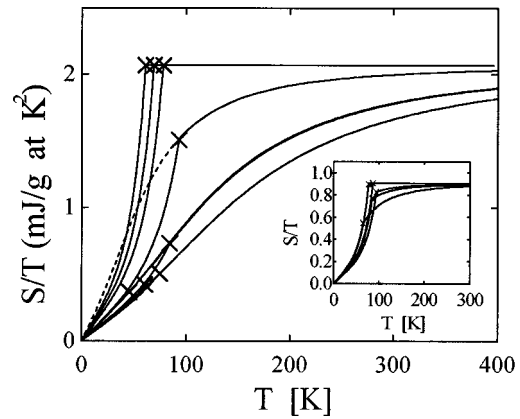


FIG. 3. The calculated temperature dependence of the electronic entropy S divided by temperature T for the five underdoped, the optimally doped, and three overdoped Bi-2212 samples as determined from Co substitution. S/T values, shown by the crosses, are determined from the Abrikosov-Gor'kov fits to the data in Fig. 2 and the curves are generated using the scaling relation using Eq. (7). The inset shows S/T determined from the Zn substituted samples.

strong depression in the entropy at and above T_c due to the appearance of the pseudogap. This indicates that, as for Y-123, the pseudogap opens in the slightly overdoped region and is already prominent at optimal doping. (iii) In the two most heavily underdoped samples another effect is evident. $(S/T)_{T_c}$ is larger than expected from the progression, lying above the lowest curves of $S/(T)/T$. This effect is observed for La-214 and Y-123 in the underdoped experimental data for S/T , γ , and χ_s commencing in all cases at the same doping state $p \leq 0.11$. This manifests itself as an intrinsic filling in of the gap and has been attributed to incipient phase separation for $0 < p < 0.11$.²⁵ (iv) It should be noted that the rate of depression of T_c with Zn content, was found to be about twice that for Co, Fe, and Ni on the overdoped side. The Zn data probably gives a better estimate of the density of states and it is likely that S/T and γ are lower than indicated in Fig. 3. Using the initial slope data for Zn (Ref. 23) we find qualitatively the same behavior as shown in Figs. 2 and 3 with a constant slope on the overdoped side yielding $S/T = \gamma = 0.91$ mJ/g atoms K^2 in the normal state, i.e., about half that found for Y-123.^{9,13} The calculated S/T data from the Zn-substituted samples is shown in the inset to Fig. 3.

In Fig. 4 we plot (solid diamonds) the p dependence of the values of E_g determined from generating the curves in Fig. 3 from the universal function given in Eq. (7). The magnitude and doping dependence of E_g is much the same as reported from NMR studies on Y-123 and Y:Ca-123 which is shown by the open diamonds. Most notably the present data are consistent with $E_g \rightarrow 0$ at $p=0.19$ as previously found in the Y-123 and Y:Ca-123 system.²⁶ Even if the Zn data are employed and lower values of E_g extracted they still interpolate to zero at $p=0.19$. Also plotted in figure (solid triangles) is the condensation energy $U_o(p)$ determined from the deduced entropy $S(T)$ by integrating the area between the extrapolated normal-state curve (exemplified in Fig. 3 by the dashed curve) and the superconducting state curve. U_o is seen to rise steeply to a maximum near $p=0.19$ where the pseudogap closes, again similar to the observed behavior for Y:Ca-123

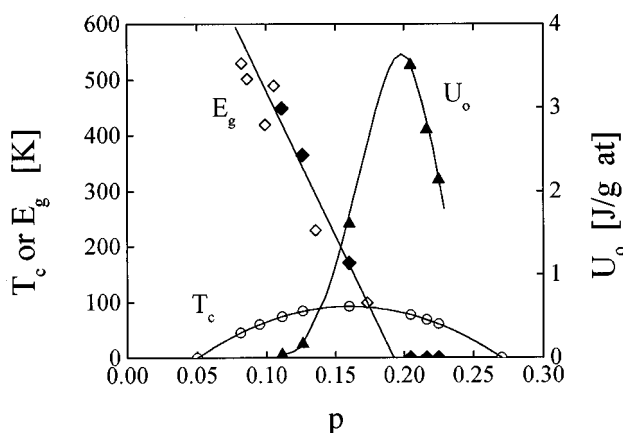


FIG. 4. T_c , pseudogap energy E_g , and condensation energy u_o , plotted as functions of hole concentration p for Bi-2212. Solid diamonds: present work; open diamonds: E_g determined from NMR studies on Y-123 and Y:Ca-123 (Refs. 10 and 11).

which peaks at 2.55 J/g atoms.^{9,13} If the Zn data are utilized lower values of U_o are obtained but a sharp peak still appears extending up to 2.2 J/g atoms. This peak in U_o is consistent with muon spin relaxation studies²⁷ of the London penetration depth, λ_L , which reveal a narrow peak in λ_L^{-2} as

a function of doping [$U_o = (3/16\pi^5)(\phi_o/\xi_o)^2\lambda_L^{-2}$, where ϕ_o is the flux quantum and ξ_o is the coherence length]. This peak has a profound influence on critical current density and irreversibility fields, as discussed elsewhere.²⁸

In conclusion, we have used the impurity suppression of T_c to determine the density of states near the Fermi level and hence S/T at T_c , then, using the scaling behavior for S/T above and below T_c the full temperature dependence of this quantity is calculated. From this all thermodynamic properties may be calculated. The results are remarkably consistent with the experimentally observed thermodynamic data for Y-123 and in particular the pseudogap energy E_g has the same doping dependence and falls to zero at $p=0.19$. The same conclusions drawn from Y-123 data therefore are preserved for Bi-2212: the pseudogap closes at a well-defined hole concentration in the lightly overdoped region; the pseudogap does not evolve from the superconducting gap but competes to the lowest temperature (as shown at the critical concentration) and the spectral gap changes slope discontinuously at T_c . We await experimental confirmation of these results by direct measurements of the electronic specific heat.

Thanks are due to Dr. J. W. Loram and Dr. G. V. M. Williams for helpful discussions. Funding by the Royal Society of New Zealand is acknowledged.

¹Z.-X. Shen and J. R. Schrieffer, Phys. Rev. Lett. **78**, 1771 (1997).

²A. G. Loeser *et al.*, Science **273**, 325 (1996).

³H. Ding *et al.*, Nature (London) **382**, 51 (1996).

⁴J. R. Cooper and J. W. Loram, J. Phys. I **6**, 2237 (1996).

⁵A special session on the pseudogap was held for the first time at the March 1997 meeting of the American Physical Society and a workshop on the pseudogap was held in May 1997 at the University of Illinois at Chicago.

⁶J. W. Loram *et al.*, *10th Anniversary HTS Workshop on Physics, Materials, and Applications* (World Scientific, Singapore, 1996), p. 341.

⁷J. W. Loram *et al.*, Physica C **235–240**, 134 (1994).

⁸J. W. Loram *et al.*, *Advances in Superconductivity VII* (Springer-Verlag, Tokyo, 1995), p. 75.

⁹J. W. Loram *et al.*, Physica C **282–287**, 1405 (1997).

¹⁰G. V. M. Williams *et al.*, Phys. Rev. Lett. **78**, 721 (1997).

¹¹J. L. Tallon, G. V. M. Williams, and J. W. Loram, in Proceedings of the Conference on Spectroscopies of Novel Superconductors [J. Phys. Chem. Solids (to be published)].

¹²J. L. Tallon *et al.* (unpublished).

¹³J. W. Loram *et al.*, Proceedings of the Conference on Spec-

troscopies of Novel Superconductors [J. Phys. Chem. Solids (to be published)].

¹⁴V. J. Emery and S. A. Kivelson, Nature (London) **364**, 434 (1995).

¹⁵M. Randeria *et al.*, Phys. Rev. Lett. **69**, 2001 (1992).

¹⁶J. L. Tallon *et al.*, Phys. Rev. Lett. **79**, 5294 (1997).

¹⁷C. Bernhard *et al.*, Phys. Rev. Lett. **77**, 2304 (1996).

¹⁸R. Lal *et al.*, Phys. Rev. B **49**, 6382 (1994).

¹⁹Y. Sun and K. Maki, Phys. Rev. B **50**, 6059 (1995).

²⁰C. Kendziora and A. Rosenberg, Phys. Rev. B **52**, R9867 (1995).

²¹M. Kang *et al.*, Phys. Rev. Lett. **77**, 4434 (1996).

²²R. D. Parks, *Superconductivity* (Marcel-Dekker, New York, 1969), Vol. 1, p. 51.

²³T. Kluge *et al.*, Phys. Rev. B **52**, R727 (1995).

²⁴J. L. Tallon *et al.*, Phys. Rev. B **51**, 12 911 (1995).

²⁵D. Obertelli, J. R. Cooper, and J. L. Tallon, Phys. Rev. B **46**, 14 928 (1992).

²⁶J. L. Tallon *et al.*, Physica C **282–287**, 236 (1997).

²⁷Ch. Niedermayer *et al.*, Phys. Rev. Lett. **71**, 1764 (1993); **72**, 2502 (1994).

²⁸J. L. Tallon, J. W. Loram, and J. R. Cooper (unpublished).